

# On Surface Order and Disorder of $\alpha$ -Pinene-Derived Secondary Organic Material

Mona Shrestha,<sup>†</sup> Yue Zhang,<sup>‡</sup> Mary Alice Upshur,<sup>†</sup> Pengfei Liu,<sup>‡</sup> Sandra L. Blair,<sup>§</sup> Hong-fei Wang,<sup>||</sup> Sergey A. Nizkorodov,<sup>§</sup> Regan J. Thomson,<sup>†</sup> Scot T. Martin,<sup>‡</sup> and Franz M. Geiger<sup>\*,†</sup>

<sup>†</sup>Department of Chemistry, Northwestern University, 2145 Sheridan Road, Evanston, Illinois 60208, United States

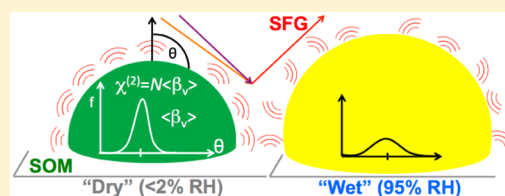
<sup>‡</sup>School of Engineering and Applied Sciences & Department of Earth and Planetary Sciences, Harvard University, 29 Oxford Street, Cambridge, Massachusetts 02138, United States

<sup>§</sup>Department of Chemistry, University of California, 1102 Natural Sciences 2, Irvine, California 92697, United States

<sup>||</sup>Environmental Molecular Sciences Laboratory, Pacific Northwest National Laboratory, 3335 Innovative Boulevard, Richland, Washington 99354, United States

## S Supporting Information

**ABSTRACT:** The surfaces of secondary organic aerosol particles are notoriously difficult to access experimentally, even though they are the key location where exchange between the aerosol particle phase and its gas phase occurs. Here, we overcome this difficulty by applying standard and sub- $1\text{ cm}^{-1}$  resolution vibrational sum frequency generation (SFG) spectroscopy to detect C–H oscillators at the surfaces of secondary organic material (SOM) prepared from the ozonolysis of  $\alpha$ -pinene at Harvard University and at the University of California, Irvine, that were subsequently



collected on Teflon filters as well as  $\text{CaF}_2$  windows using electrostatic deposition. We find both samples yield comparable SFG spectra featuring an intense peak at  $2940\text{ cm}^{-1}$  that are independent of spectral resolution and location or method of preparation. We hypothesize that the SFG spectra are due to surface-active C–H oscillators associated with the four-membered ring motif of  $\alpha$ -pinene, which produces an unresolvable spectral continuum of approximately  $50\text{ cm}^{-1}$  width reminiscent of the similar, albeit much broader, O–H stretching continuum observed in the SFG spectra of aqueous surfaces. Upon subjecting the SOM samples to cycles in relative humidity (RH) between  $<2\%$  RH and  $\sim 95\%$  RH, we observe reversible changes in the SFG signal intensity across the entire spectral range surveyed for a polarization combination probing components of the vibrational transition dipole moments that are oriented parallel to the plane of incidence, but no signal intensity changes for any other polarization combination investigated. These results support the notion that the C–H oscillators at the surfaces of  $\alpha$ -pinene-derived SOM deposited on  $\text{CaF}_2$  windows shift back and forth between two different molecular orientation distributions as the RH is lowered (more ordered) or raised (less ordered). The findings thus point toward the presence of a reversible surface switch for hindering (more ordered,  $<2\%$  RH) and promoting (less ordered,  $\sim 95\%$  RH) exchange between the aerosol particle phase and its gas phase.

## I. INTRODUCTION

The propensity of atmospheric organic particles to undergo growth and participate in chemical reactions is thought to be influenced by the ambient relative humidity (RH).<sup>1–4</sup> Specifically, water has been proposed to act as a plasticizer,<sup>3</sup> with its presence leading to decreases in the viscosity of secondary organic material (SOM) by orders of magnitude under high compared to low RH. By means of illustration, one can think of SOM as either “marble-like” under low RH, “honey-like” under intermediate RH, and “liquid-like” under saturated conditions.<sup>1,2</sup> Given the importance of organic particles in the climate system,<sup>4–14</sup> and the dynamic nature of relative humidity in most environmental settings,<sup>15,16</sup> it is reasonable to consider SOM as suspended nanoscale reaction vessels in which atmospherically significant chemical and physical processes can occur for time durations dictated by the material viscosity. Compounds formed inside the particles under high RH conditions are therefore expected to be “locked

in” under low RH conditions until the RH rises again, effectively turning organic particles under low RH conditions into time capsules of chemical composition, with high and low RH acting as a switch. Likewise, reports of increased ozonolysis of C=C double bond containing species with increasing RH<sup>17</sup> and further increased reactivity in the presence of water<sup>18</sup> point toward the possibility that RH-dependent changes of SOM properties may influence heterogeneous reactions as well.

Here, we hypothesize that particles transitioning from “marble-like” to “honey-like” present molecules to the external world that are subject to RH-dependent differences in molecular orientation distributions. Similar to reports of orientation-dependent heterogeneous reactions of olefin stereo-

**Special Issue:** Mario Molina Festschrift

**Received:** October 27, 2014

**Revised:** December 16, 2014

**Published:** December 16, 2014

isomers,<sup>19,20</sup> such differences could influence heterogeneous processes occurring at the particle surfaces, and subsequently the particle interior. Reflecting on this situation is important, as one could consider interfacial environments characterized by highly oriented C–H groups as largely impenetrable to gas phase species, while a disordered array of C–H groups may permit more efficient surface accommodation and absorption into the bulk.<sup>21–23</sup>

While it is currently not possible to selectively probe the surfaces of suspended particles under ambient conditions using molecular spectroscopy, one can do so by applying vibrational sum frequency generation (SFG) spectroscopy to particles immobilized on Teflon filters or optical windows. Using this approach, we have provided the first molecular spectra of SOM,<sup>14,24–25</sup> identified trans- $\beta$ -IEPOX to be the majority species on the surfaces of isoprene-derived SOM,<sup>26</sup> and reported 20 ng per filter limits of detecting  $\alpha$ -pinene-derived SOM.<sup>27</sup> SFG spectroscopy is also a well-established surface analysis method for determining molecular orientation distributions of organic ligands on nanomaterials<sup>28–32</sup> and of organic materials undergoing phase transitions<sup>33</sup> or being submersed in environments of varying dielectric constant.<sup>34</sup> For instance, Shen and co-workers reported spectral intensity reductions in the methylene C–H stretching region upon freezing eicosane (C<sub>20</sub>H<sub>42</sub>) and attributed this observation to a reduction in gauche (–CH<sub>2</sub>–CH<sub>2</sub>–) defects.<sup>33</sup> Concomitant with this change in the SFG spectra was a substantial SFG signal increase in the methyl C–H stretching region, consistent with an increase in molecular order upon freezing of eicosane. Likewise, Chen and co-workers reported SFG spectra from C–H oscillators on polymer side chains that identify changes in their molecular orientation as the polymer is placed in water versus air.<sup>34</sup> Most recently, Richmond and co-workers<sup>35</sup> clearly showed increases in the SFG signal intensities from C–H stretches of a charged polymer as the extent of molecular order within the surface-localized polymer increased by the addition of Ca<sup>2+</sup> ions.

Our current study presents the first RH-dependent vibrational SFG spectra obtained from the surfaces of  $\alpha$ -pinene-derived SOM deposited on as well as transferred on to optical windows and reports that “marble-like”<sup>1,2</sup> and “honey-like”<sup>1,2</sup> SOMs present more ordered and less ordered C–H oscillators, respectively, to the external world. We find fully reversible changes in the SFG responses as we subject the SOM to < 2% RH and ~95% RH and discuss the atmospheric implications of our findings in the context of the propensity of atmospheric organic particles to undergo particle growth, participate in chemical reactions, and cloud condensation nuclei (CCN) activity.

## II. EXPERIMENTAL SECTION

**II.1.  $\alpha$ -Pinene-Derived SOM.** Aerosol particles were prepared by ozonolysis of the volatile precursor  $\alpha$ -pinene in a flow tube reactor at Harvard University<sup>27</sup> and in a smog chamber at the University of California, Irvine.<sup>36</sup> At the Harvard flow tube reactor,  $\alpha$ -pinene and ozone were injected via two different inlets into a flow tube maintained at ambient temperature and pressure under conditions that can lead to condensational and coagulative growth. The particles were grown without seed particles and ranged in mode diameters from 35 to 105 nm, depending under what conditions they were prepared and collected. The aerosol particles were collected on Teflon filters following our previously published

methods, with a collection efficiency of 98%.<sup>14,24,26,27</sup> In the chamber case, a SOM particle sample was prepared from 137 ppb of (–)- $\alpha$ -pinene and 400 ppb of ozone and collected on a Teflon filter (Whatman, 46.2 mm diameter, part # 7592-104) for about 34 minutes using a home-built Teflon impactor. The smog chamber has been described in detail previously.<sup>36</sup> Additionally, an electrostatic precipitator (TSI 3089) at Harvard was employed in this work in order to distribute aerosol particles uniformly on CaF<sub>2</sub> optical windows (ISP Optics), which were used directly for the spectroscopic analyses.<sup>37</sup> The window was placed on the high voltage electrode of the electrostatic precipitator; particles charged by the neutralizer were deposited for 30 min to 2 h onto the substrate with a flow rate of 2 L min<sup>–1</sup>. The CaF<sub>2</sub> windows were first cleaned in methanol and then in Millipore water and dried in an oven, followed by a plasma cleaner (Harrick Plasma) at Northwestern, and using a UV/ozone cleaner (Windsor Scientific, model ProCleaner-Plus) at Harvard, to avoid contamination with organic species deposited from lab air. The SOM-containing Teflon filters collected at Harvard, on the other hand, were pressed by hand against clean CaF<sub>2</sub> optical windows to transfer SOM onto them, followed by removal of the filter from the windows and subsequent analysis. The mass of the particles collected on the filter was estimated by using the following equation:

$$m = ft\eta c_{\text{mass}} \quad (1)$$

Here,  $f$  is flow rate,  $t$  is collection time,  $\eta$  is collection efficiency, and  $c_{\text{mass}}$  is the particle mass concentration obtained from a scanning mobility particle sizer, assuming a particle density of 1200 kg m<sup>–3</sup> and a collection efficiency near unity. Table SI in the Supporting Information lists the pinene and ozone concentration used for preparing the SOM (at Harvard) for the samples studied here for relative humidity experiments, the particle collection time, and whether the particles were collected on a Teflon filter or an optical window.

**II.2. Relative Humidity Flow Cell and SFG Experiments.** The SOM-deposited and SOM-pressed windows were used in a home-built relative humidity (RH)-controlled flow system (Figure 1A). We sent helium gas across the SOM-containing optical windows via a dry and a humidified flow line, with the latter consisting of a bubbler containing Millipore water. Mass flow controllers (MKS, model no. M100B14CS1BN) connected to an A/D converter (MKS, type 247) were used to regulate the helium flow through the two lines under the constraint of constant He flow such that a desired RH value, measured by a calibrated RH meter (Omega Engineering, RH-USB, 2% to 98% RH range, uncertainty of  $\pm 3$  percentage points), was reached. Measured relative humidity values of 91% to 95%, termed “wet”, and below 2%, termed “dry”, were employed in this study, and RH jumps between these values took about 2 min using our sample cell, which had an internal volume of approximately 7 cm<sup>3</sup>.

Our previous studies have shown SFG to be a nondestructive and a sensitive technique for analyzing nanogram amounts of SOM under ambient conditions.<sup>14,24,27</sup> For the samples studied here, we employed standard resolution (10–15 cm<sup>–1</sup>) SFG spectroscopy and directed a broadband infrared and a visible beam through the CaF<sub>2</sub> window at incident angles of 60° and 45°, respectively, and overlapped them in time and space to generate SFG signals that oscillated at the sum of the two input frequencies (Figure 1B). After accounting for refraction of the beams through the CaF<sub>2</sub> window, the incident angles of

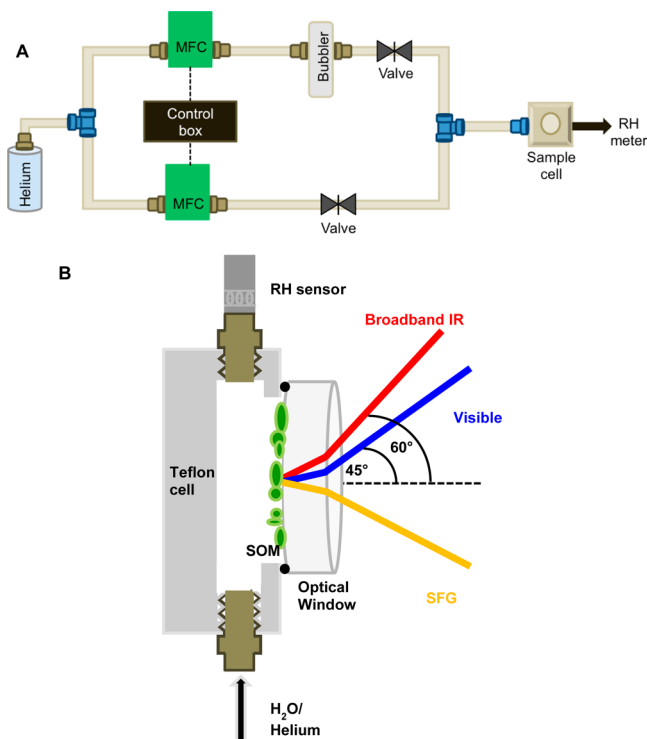


**Figure 1.** Experimental setup. Panel A shows the flow/RH control system. Panel B shows the SFG cell geometry.

infrared and visible beams at the SOM/CaF<sub>2</sub> interface were 38° and 30°, respectively. The infrared light field was tuned to the C–H stretching region to probe the SFG signal arising from the C–H oscillators located at the SOM/air interface, with negligible signal contributions from internal interfaces, should any exist within the particles.<sup>38</sup> Given that the Fresnel coefficients that determine how many SFG signal photons are transmitted from the interface to the detector depend on the difference in refractive index, the SFG signal detected here was mostly due to the interfacial regions characterized by the largest refractive index changes, which was the interface between the gas phase and the particle material on the window.

We collected the SFG spectra using the ssp (*s* = light field plane-polarized perpendicular to the plane of incidence, *p* = light field plane-polarized parallel to the plane of incidence, listed in the order of the SFG, the upconverter, and the infrared frequencies) polarization combination to probe those vibrational mode components that were orientated parallel to the plane of incidence. ppp-Polarized SFG spectra were recorded as well to probe for molecular orientation changes. A complete description of the standard (10–15 cm<sup>-1</sup>) and sub-1 cm<sup>-1</sup> resolution SFG spectrometers used here was provided earlier.<sup>14,24,27,39,40</sup> The main difference between the 10–15 cm<sup>-1</sup> resolution and the sub-1 cm<sup>-1</sup> resolution SFG spectra is that the latter can provide a nearly intrinsic spectral line shape and can resolve much finer spectral features if any are present.<sup>41</sup> The sub-1 cm<sup>-1</sup> resolution SFG spectra were collected with the incident angles of infrared and visible incident angles on the CaF<sub>2</sub> window at 55° and 45°, respectively.

The square root of the SFG signal intensity,  $I_{\text{SFG}}$ , is proportional to the SFG electromagnetic field,  $E_{\text{SFG}}$ , which is equal to the second order nonlinear susceptibility,  $\chi^{(2)}$ , and the energies of the incident upconverter pulse,  $E_{\omega}$ , and the infrared,  $E_{\nu}$ .<sup>42–45</sup> The second order nonlinear susceptibility depends on

the number of SFG-active C–H oscillators on the SOM surface,  $N_{\text{surf}}$  and the average molecular orientation distribution of their molecular hyperpolarizability,  $\beta_{\text{C-H}}$ , according to

$$\sqrt{I_{\text{SFG}}} \propto E_{\text{SFG}} = \chi^{(2)} E_{\omega} E_{\nu} = N_{\text{surf}} \langle \beta_{\text{C-H}} \rangle E_{\omega} E_{\nu} \quad (2)$$

Given that the visible pulse energy was less than 1 μJ and held constant, and given that the number of SOM-containing particles in the laser spot was constant under most conditions (*vide infra* for exceptions), any changes in the SFG spectra were attributable to changes in the average molecular orientation distribution of the C–H oscillators at the SOM surface. ssp-Polarized SFG spectra were collected for a given SOM sample at a particular RH value for at least 10 min, with each spectral acquisition time lasting 2 min. The acquisition time for each ppp-polarized spectrum was 4 min long. Following our previously described data workup procedures,<sup>14,24,27</sup> we report here the average of five SFG spectra for each RH condition (wet or dry).

**II.3. Characterization by Atomic Force Microscopy (AFM) and Raman Spectroscopy under Ambient Conditions.** AFM imaging was carried out in tapping mode using a Dimension FastScan atomic force microscope. A 10 μm × 10 μm section of the sample was scanned at a rate of 1 Hz. Height mode images of a clean CaF<sub>2</sub> window and a window containing SOM collected using the Harvard flow tube for about 7 h by electrostatic precipitation shown in Figure 2 clearly demonstrate the presence of individual particles that have dimensions expected for condensationally grown particles.

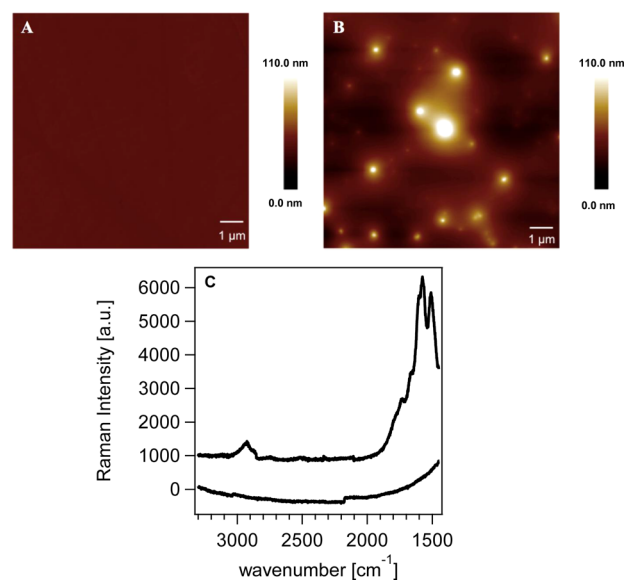


**Figure 2.** AFM and Raman data. Panels A and B show AFM images of a clean window and a window containing deposited particles, respectively. Panel C shows Raman spectra of a blank CaF<sub>2</sub> window (bottom) and the deposited material (top); spectra are offset for clarity.

Raman spectra were collected using an Acton TriVista Confocal Raman System (Princeton Instruments), which employs a 514.5 nm gas laser. A particle sample prepared from the ozonolysis of a 50:50 mix of (+) and (–)- $\alpha$ -pinene and collected for ~10 h by electrostatic precipitator on a CaF<sub>2</sub> window was placed on the sample stage, and the laser beam was focused onto it using a 10× objective lens. The Raman signal

was then dispersed using a triple spectrograph (Acton) and detected with a liquid-nitrogen-cooled charged coupled device. Spectra were acquired for 1 min from 1450 to 3300  $\text{cm}^{-1}$ , calibrated to poly(methyl methacrylate) (PMMA) and background subtracted. Figure 2C shows Raman spectrum for a blank  $\text{CaF}_2$  window (bottom) while the top spectrum in the same figure shows that most of the spectral intensity for the SOM occurs in the carbonyl stretching region and the C–H stretching region is associated with approximately 10 times lower signal intensity when compared to the carbonyl stretching region, and that aromatic or vinylic C–H stretches, expected above 3000  $\text{cm}^{-1}$ , are not observed.

### III. RESULTS

Figure 3 shows the SFG spectrum of  $\alpha$ -pinene-derived SOM collected using the Harvard flow tube reactor and recorded

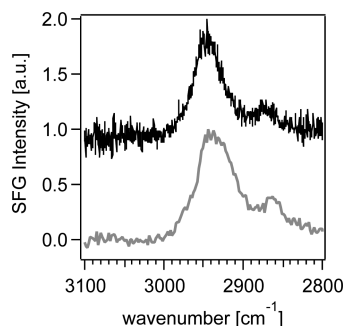


**Figure 3.** ssp-Polarized SFG spectra of secondary organic material prepared from the ozonolysis of  $\alpha$ -pinene using the UC Irvine smog chamber (top) and the Harvard flow tube reactor (bottom). The spectra are collected using a  $\text{CaF}_2$  window and recorded using standard (10–12  $\text{cm}^{-1}$ , bottom) and sub-1  $\text{cm}^{-1}$  (top) spectra resolution at Northwestern University (bottom) and Pacific Northwest National Laboratory (top). Spectra are normalized to their maximum SFG intensity and offset by 1.0 for clarity.

using Northwestern’s SFG spectrometer matches the one from the  $\alpha$ -pinene-derived SOM collected using the Irvine smog chamber (as stated in section II.1. that was recorded with a sub-1  $\text{cm}^{-1}$  spectral resolution SFG spectrometer located at Pacific Northwest National Laboratory (PNNL). The SOM sample used here from Harvard was prepared under the same reaction conditions as listed for Sample 1 in Table S1 but collected for 265 minutes. In both SFG experiments, the SOM sample on a Teflon filter had been pressed against a  $\text{CaF}_2$  window. Similar to our prior reports,<sup>14,24,27</sup> the SFG spectra show a dominant peak between 2930 and 2950  $\text{cm}^{-1}$  and a small peak between 2850 and 2870  $\text{cm}^{-1}$  for both spectral resolutions. Just like the Raman spectra, signals above 3000  $\text{cm}^{-1}$ , which would indicate the presence of aromatic or vinylic C–H stretches, are not observed. SFG spectra collected at both NU and PNNL are qualitatively similar to the Raman spectrum (see Figure S1). Unlike the case for pure  $\alpha$ -pinene adsorbed on the  $\text{CaF}_2$  or  $\text{SiO}_2$  windows, whose sub-1  $\text{cm}^{-1}$  resolution spectra contains 10 well resolved spectral features in the 2800–3000  $\text{cm}^{-1}$  region, the 1  $\text{cm}^{-1}$  resolution spectrum of the  $\alpha$ -pinene-derived SOM sample shows broad spectral features that cannot be resolved nearly as clearly as the adsorbed pure  $\alpha$ -pinene.<sup>46</sup> As we discuss below, this result may be a reflection of considerable chemical complexity of the  $\alpha$ -pinene-derived SOM sample resulting in a large number of chemically different species contributing to the band shape on the one hand, or spectrally

broad contributions of the oscillators of just a few surface-active species on the other. This latter situation is reminiscent of what is observed for SFG spectra of aqueous surfaces, whose complexity is due to coupled oscillators of just one molecular species, namely water.<sup>44,47,48</sup> Given the similarity in the two spectra, and despite their dramatically different spectral resolving power,<sup>41</sup> we conclude that the standard resolution of the Northwestern University SFG system is appropriate for analyzing the surfaces of  $\alpha$ -pinene-derived SOM and further that SOM prepared at Harvard and Irvine produce comparable SFG spectra.

Figure 4 shows the SFG spectra obtained from SOM sample 1 (Table Supporting Information) on a  $\text{CaF}_2$  window, which

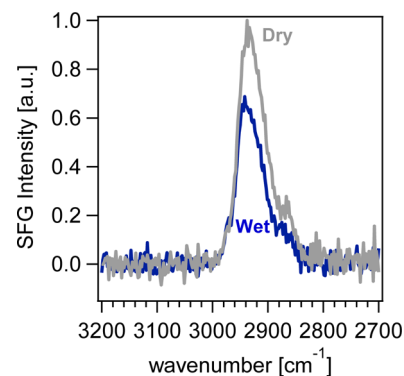


**Figure 4.** ssp-Polarized SFG spectra of sample 1 collected in “narrow-band” mode during exposure to <2% RH (gray) and ~95% RH (blue).

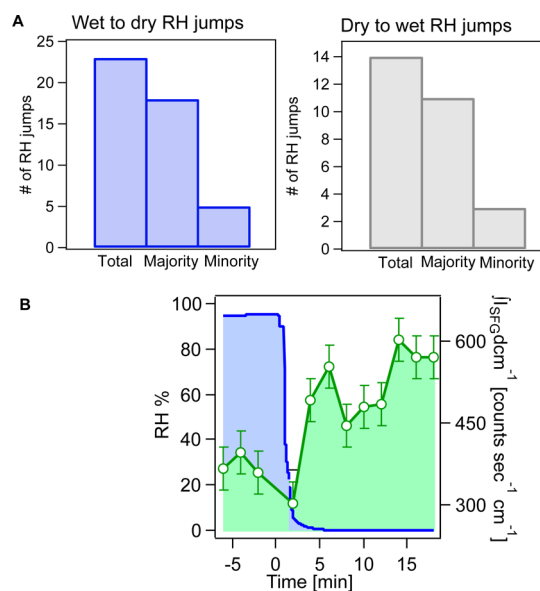
was collected on a Teflon filter using the Harvard flow tube, then pressed against the window and subsequently removed from the filter. In contrast to the spectra shown in Figure 3, where the entire IR range shown in the  $x$ -axis was covered by the incident IR light, the spectrum shown in Figure 4 was collected by centering the spectral range of the IR light around 2940  $\text{cm}^{-1}$  with a bandwidth of approximately 120  $\text{cm}^{-1}$  to cover the strong and weak modes at 2940 and 2870  $\text{cm}^{-1}$ . The advantage of this approach is that the spectrum can be recorded in 2 min, whereas covering the entire spectral range of the C–H stretching region takes about 10 times longer. Below, we use this “narrow-band” approach as the 2 min spectral acquisition times enable us to track the SFG response during RH jumps in close to real time.

Figure 4 shows that ssp-polarized SFG signal intensity decreases in the narrow-band spectral range probed upon increasing the RH from <2% to 95% RH. Under “wet” conditions, the SFG signal from the O–H oscillators of water molecules adsorbed to the SOM surface could interfere destructively with the C–H oscillators of the SOM surface species, thus leading to the observed SFG signal intensity reductions at high RH. Such spectral interference has been reported for a variety of air/water interfaces containing surfactant monolayers.<sup>49,50</sup> We thus replaced the water in the bubbler with deuterium oxide and repeated RH experiments using the RH meter calibrated for  $\text{H}_2\text{O}$ . Given that  $\text{D}_2\text{O}$  has a slightly lower saturation vapor pressure (2.0 kPa) than water (2.3 kPa) at 20  $^\circ\text{C}$ ,<sup>51,52</sup> the  $\text{D}_2\text{O}$  experiments were carried out at 86% to 91% (as read by the RH meter). The SFG responses observed for  $\text{H}_2\text{O}$  persist when using  $\text{D}_2\text{O}$ ; the average percent increase (from 6 high to low RH jumps) in the integral of the SFG signal intensity computed from 3200  $\text{cm}^{-1}$  to 2700  $\text{cm}^{-1}$  for two different particle samples is 21% (range: 12% to 30%)

while the average percent decrease (from 3 low to high RH jumps) is 27% (range: 20% to 32%). Only those RH jumps showing "majority response" (discussed later in this section) are employed in the above calculations. These results provide conclusive evidence that change in the SFG signal intensities are not due to spectral interference between O–H/O–D and C–H oscillators at the SOM surface (see Figure SII).

As a second important control, we calculated if possible changes in the refractive index of air could influence the magnitudes of the Fresnel coefficients, which are the optical parameters that quantify the amount of light entering and exiting the surface region in an SFG experiment. The refractive indices based on Ciddor equation of air at 633 nm and 20 °C are 1.000271800 and 1.000267394 at 0% RH and 100% RH, respectively (see Table SII).<sup>53</sup> Liu et al. reported a refractive index for pinene-derived SOM of 1.49–1.52 at 550 nm.<sup>37</sup> By employing Snell's law of refraction<sup>54</sup> and by calculating the Fresnel coefficients<sup>55</sup> at 100% and 0% RH using the known refractive index values, we estimate the ratio of the ssp-polarized SFG intensities at high RH and low RH to be close to 1.00, indicating that refractive index changes in air for the two different RH conditions are not large enough to rationalize the differences in the SFG signal intensities observed in Figure 4. We conclude from these control studies that the observed changes in the SFG signal intensity that occur when SOM is subjected to dry versus wet conditions are due to changes in the molecular orientation distributions of the various SFG-active C–H oscillators.

Given that no new spectral features appear upon changing RH conditions in our experiments, we integrate the SFG signal intensity from 3200  $\text{cm}^{-1}$  to 2700  $\text{cm}^{-1}$  to determine the change in the SFG response for 37 RH jumps, while reducing the effect of noise in the SFG spectra. Of 23 "wet" to "dry" and 14 "dry" to "wet" RH jumps for 4 different particle samples (Table SI), 29 lead to a change of at least 10% in the SFG response irrespective of the jump direction. This type of response is termed as the "majority response" provided the integrated value under "dry" RH is greater than that under "wet" RH. For those RH jumps exhibiting a "majority response", the average percent increase in the integral of the SFG signal intensity and its standard deviation calculated from 18 "wet" to "dry" RH jumps is  $47 \pm 19\%$  while the average percent decrease in the integral value and its standard deviation estimated from 11 "dry" to "wet" jumps is  $38 \pm 11\%$ . The average percent increase and decrease computed for the RH jumps that showed "majority response" using the maximum peak intensity at  $\sim 2940 \text{ cm}^{-1}$  as opposed to the integral between 3200  $\text{cm}^{-1}$  and 2700  $\text{cm}^{-1}$  are statistically identical, namely  $41 \pm 20\%$  and  $34 \pm 13\%$ , respectively. For the purpose of this paper, we focus on the integral values. Furthermore, SFG signal changes of less than 10%, irrespective of the jump direction, and larger integral values at "wet" RH compared to "dry" RH are considered "minority responses". As shown in Figure 5A, only 5 of the 23 "wet" to "dry" jumps and 3 of the 14 "dry" to "wet" jumps exhibit a "minority response". Time-dependent experiments (Figure 5B) show the change in the SFG "majority response" is instantaneous in terms of the fastest spectral acquisition time we employed (2 minutes). As shown in the Supporting Information (Figure SIII), the ppp-polarized SFG spectra show no signal intensity change upon changing RH, irrespective of whether ssp-polarized response fall into the "majority response" or "minority response" category.



**Figure 5.** (A) Total number of SFG experimental outcomes resulting in the majority and the minority response for RH jumps from wet to dry (left) and dry to wet (right) conditions. (B) Time-dependent experiment conducted that shows the increase in signal intensity as the RH is transitioned from  $\sim 95\%$  to  $<2\%$ .

#### IV. DISCUSSION AND ATMOSPHERIC IMPLICATIONS

Equation 2 indicates that there may be two causes for any observed change in the SFG signal intensity of a system of C–H oscillators. First, we consider the number of C–H oscillators probed by our system. Given that the number of particles remains constant in the experiments, and assuming that organic material does not get lost from a given particle during the humidification-drying cycles, we can consider the total number of C–H oscillators per particle to remain constant. To estimate how many of the oscillators present at the surface of a dry particle remain at the interface upon humidification we have to account for the hygroscopic growth of the particle. As shown in Figure 6, the total number of C–H oscillators per particle does

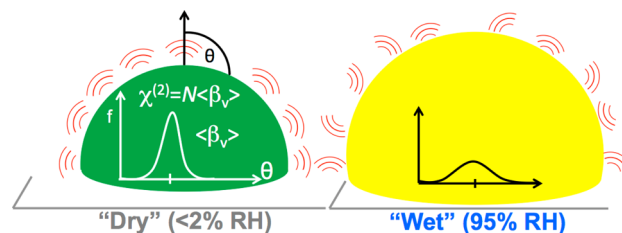


**Figure 6.** Cartoon representation of RH-dependent changes in orientation distributions of C–H oscillators at the surfaces of SOM studied in this work used to rationalize the majority response of the SFG spectra. SFG-active oscillators are represented in red, and the assumption is that their number at the interface does not decrease under elevated RH conditions.

not change during the hygroscopic growth but the particle volume and the exposed surface area both increase. The published hygroscopic growth factors for  $\alpha$ -pinene-derived SOM range from 1.05 to 1.12 at 95% RH,<sup>56,57</sup> leading to a potential reduction in the density of the C–H oscillators by a factor ranging from 1.16 to 1.40 under wet conditions when compared to dry conditions. However, it is probably incorrect

to assume that the number of the C–H oscillators in the SFG-probed surface layer should drop by the same factor because the surface-active  $\alpha$ -pinene oxidation products may cover the surface nearly as densely as they do in a dry particle. Along the same line of thought, increased water content in the particles is unlikely to drive surfactant-like compounds from the particle bulk to the surface when compared to dry conditions, as that scenario would result in SFG signal increases at high versus low RH. Conversely, if the increased water content in the SOM under “wet” conditions was to result in the displacement of organic species from the SOM surface, where they are SFG active, to the SOM interior, where they would be SFG inactive, the resulting SFG signal intensity decreases would occur across all polarization combinations surveyed. This scenario is unlikely as the ppp-polarized SFG spectra, shown in the Supporting Information (Figure XIII), do not change as the RH is cycled between  $\sim 95$  and  $<2\%$ .

The second factor in eq 2 describes the molecular orientation distributions of the SFG active C–H oscillators. Given that the SFG signal intensity reductions are generally associated with increased surface disorder and concomitant loss in net polar alignment of oscillators under conditions of mass conservation, we attribute the SFG signal decreases observed under dry versus wet conditions to substantial changes in SOM surface disorder.<sup>58</sup> This interpretation of our observations is supported by reports of marble- versus honey-like properties of SOM, in terms of its viscosity, under low versus high RH conditions.<sup>1,2</sup> Under this interpretation, well-ordered SFG-active C–H oscillators are described by a narrow molecular orientation distribution of the molecular hyperpolarizability tensor,  $\beta$ , under dry conditions, whereas wet conditions broaden the orientation distribution, and thus lower the second order susceptibility,  $\chi^{(2)}$  (Figure 6). A broadening of the molecular orientation distribution could also coincide with a shift to higher or lower angles in the whole distribution when compared to the narrow orientation distributions; both possibilities would lead to decreased SFG signal intensity under wet conditions. The observation of ssp-polarized SFG spectra that change intensity with RH in a fully reversible fashion while the ppp-polarized SFG spectra remain invariant with RH indicates for the vast majority of the experimental outcomes that the C–H oscillators of  $\alpha$ -pinene-derived SOM deposited on CaF<sub>2</sub> windows switch back and forth between two different molecular orientation distributions in a reversible fashion as the RH is lowered or raised. Rationalizing our observations requires more detailed knowledge about how the SOM shape and location on the CaF<sub>2</sub> windows change with RH. To this end, future studies will focus on interfacing our tapping mode AFM instrument with an RH controlled cell, and we will report results from those studies in due course.

In conclusion, we have shown that SOM prepared from the ozonolysis of  $\alpha$ -pinene and collected on Teflon filters at the Harvard flow reactor and at the Irvine smog chamber produce comparable SFG spectra in the C–H stretching region. This result indicates that the surfaces of both types of SOM are comparable, at least as viewed by SFG spectroscopy. Yet, the finding that the SFG spectra are comparable even when probed with at least 10 times improved spectral resolution compared to standard resolution SFG spectroscopy indicates that the SFG responses of the C–H oscillators at the surfaces of the SOM studied here are too congested to be resolved. This finding is in stark contrast to the sub-1 cm<sup>-1</sup> resolution SFG spectroscopy of  $\alpha$ -pinene vapor in contact with a CaF<sub>2</sub> window, which is

much richer in information content than its standard-resolution SFG spectrum<sup>46</sup> and is dominated by one sharp peak at 2930.9  $\pm$  0.1 cm<sup>-1</sup> that features a bandwidth of just 1.40  $\pm$  0.04 cm<sup>-1</sup>, and a second contribution at 2939.1  $\pm$  0.2 cm<sup>-1</sup> that exhibits a bandwidth of just 0.59  $\pm$  0.07 cm<sup>-1</sup>. The question then arises why the spectral features in the SFG spectra are not resolvable, even when using the highest spectral resolution available in SFG spectroscopy to date. This question highlights the need for spectroscopic studies of SOM constituents, including compounds featuring the four-membered rings often reported in mass spectroscopic studies<sup>9,59,60</sup> that may be further linked through ester and/or anhydride bridge motifs to form so-called extremely low-volatility organic compounds consisting of C<sub>20</sub> compounds.<sup>61,62</sup> Preliminary results indicate that SOM formed from  $\alpha$ -pinene, which we deuterated to spectroscopically silence two of its three methyl groups, shows no significant changes in the SFG responses, indicating that the SFG signals are due to other C–H oscillators. These oscillators appear to produce a 50 cm<sup>-1</sup> broad continuum that is reminiscent of the similar, albeit much broader, O–H stretching continuum observed in the SFG spectra of aqueous surfaces that is caused by a variety of intra- and intermolecular interactions among the oscillators of a single molecular species (H<sub>2</sub>O).<sup>48</sup>

All the work presented here supports the notion that the C–H oscillators of  $\alpha$ -pinene-derived SOM deposited on CaF<sub>2</sub> windows switch back and forth between two different molecular orientation distributions in a reversible fashion as the RH is lowered or raised. The orientation distribution at high RH, along with the possible decrease in C–H oscillator density (but not number) per particle, is likely to represent a less dense arrangement of organic compounds at the particle surface, through which the transfer of molecular species exchanging between the aerosol particle phase and its gas phase is more facile at 95% RH when compared to  $<2\%$  RH. This situation is similar to reports of extensive CO adsorption to dendrimer encapsulated Pt nanoparticles when they are present in a liquid versus gas phase<sup>63</sup> and is likely to be applicable to other classes of atmospheric aerosol particles as well, including sea spray aerosol.<sup>64,65</sup> The absence of a reliable and definite assignment of the SFG spectral features currently precludes an analysis regarding molecular orientation angles and their distributions from the ratio of the SFG amplitudes obtained from the ssp- and ppp-polarized spectra. Likewise, the 50 cm<sup>-1</sup> broad continuum that cannot be resolved even with the best currently available spectral resolution (sub-1 cm<sup>-1</sup>) remains enigmatic. However, access to deuterated  $\alpha$ -pinene, from which deuterium-labeled SOM can be prepared, will allow us to take steps toward understanding the SFG responses of SOM, which will be reported in due course.

## ■ ASSOCIATED CONTENT

### 📄 Supporting Information

Table listing sample collection conditions, table consisting of refractive indices of air at 0% and 100% RH, SFG and Raman spectra collected for  $\alpha$ -pinene derived SOM, ssp-polarized SFG spectra for RH experiments with D<sub>2</sub>O and H<sub>2</sub>O showing negligible interference from O–D/O–H stretches, and ppp-polarized SFG spectra for “dry” and “wet” conditions. This material is available free of charge via the Internet at <http://pubs.acs.org>.

## ■ AUTHOR INFORMATION

## Corresponding Author

\*E-mail: geigerf@chem.northwestern.edu.

## Notes

The authors declare no competing financial interest.

## ■ ACKNOWLEDGMENTS

M.S. gratefully acknowledges support from an ISEN Sustainability Fellowship. This work is supported by the National Science Foundation (NSF) Environmental Chemical Sciences Program in the Division of Chemistry under Grant No. 1111418. Raman experiments in this work were conducted in the Keck-II facility of NUANCE Center at Northwestern University, which is supported by NSEC (NSF EEC-0647560), MRSEC (NSF DMR-1121262), the Keck Foundation, the State of Illinois, and Northwestern University. M.S. thanks Alicia McGeachy and Laura Olenick for their help with Raman spectroscopy. M.S. would also like to acknowledge Gajendra Shekhawat (from NIFTI facility of NUANCE Center) for his guidance with the AFM studies. M.S. thanks Dr. Jennifer Achtyl and Hilary Chase for their help with Fresnel coefficient calculations. The UC Irvine team acknowledges support from NSF Grant AGS-1227579. Part of this work was conducted at the William R. Wiley Environmental Molecular Sciences Laboratory (EMSL), a national scientific user facility located at the Pacific Northwest National Laboratory (PNNL) and sponsored by the Department of Energy's Office of Biological and Environmental Research (BER). M.A.U. and H.F.W. thank Dr. Li Fu for his help while taking the high-resolution SFG data.

## ■ REFERENCES

- (1) Koop, T.; Bookhold, J.; Shiraiwa, M.; Poeschl, U. Glass Transition and Phase State of Organic Compounds: Dependency on Molecular Properties and Implications for Secondary Organic Aerosols in the Atmosphere. *Phys. Chem. Chem. Phys.* **2011**, *13*, 19238–55.
- (2) Renbaum-Wolff, L.; Grayson, J. W.; Bateman, A. P.; Kuwata, M.; Sellier, M.; Murray, B. J.; Shilling, J. E.; Martin, S. T.; Bertram, A. K. Viscosity of  $\alpha$ -Pinene Secondary Organic Material and Implications for Particle Growth and Reactivity. *Proc. Natl. Acad. Sci. U.S.A.* **2013**, *110*, 8014–19.
- (3) Kidd, C.; Perraud, V.; Wingen, L. M.; Finlayson-Pitts, B. J. Integrating Phase and Composition of Secondary Organic Aerosol from the Ozonolysis of  $\alpha$ -Pinene. *Proc. Natl. Acad. Sci. U.S.A.* **2014**, *111*, 7552–7.
- (4) Hallquist, M.; Wenger, J. C.; Baltensperger, U.; Rudich, Y.; Simpson, D.; Claeys, M.; Dommen, J.; Donahue, N. M.; George, C.; Goldstein, A. H.; et al. The Formation, Properties and Impact of Secondary Organic Aerosol: Current and Emerging Issues. *Atmos. Chem. Phys.* **2009**, *9*, 5155–236.
- (5) Kroll, J. H.; Seinfeld, J. H. Chemistry of Secondary Organic Aerosol: Formation and Evolution of Low-Volatility Organics in the Atmosphere. *Atmos. Environ.* **2008**, *42*, 3593–624.
- (6) Chan, A. W. H.; Chan, M. N.; Surratt, J. D.; Chhabra, P. S.; Loza, C. L.; Crounse, J. D.; Yee, L. D.; Flagan, R. C.; Wennberg, P. O.; Seinfeld, J. H. Role of Aldehyde Chemistry and NO<sub>x</sub> Concentrations in Secondary Organic Aerosol Formation. *Atmos. Chem. Phys.* **2010**, *10*, 7169–88.
- (7) Lee, S.; Kamens, R. M. Particle Nucleation from the Reaction of [ $\alpha$ ]-Pinene and O<sub>3</sub>. *Atmos. Environ.* **2005**, *39*, 6822–32.
- (8) Tolocka, M. P.; Heaton, K. J.; Dreyfus, M. A.; Wang, S.; Zordan, C. A.; Saul, T. D.; Johnston, M. V. Chemistry of Particle Inception and Growth During  $\alpha$ -Pinene Ozonolysis. *Environ. Sci. Technol.* **2006**, *40*, 1843–8.
- (9) Gao, Y.; Hall, W. A., IV; Johnston, M. V. Molecular Composition of Monoterpene Secondary Organic Aerosol at Low Mass Loadings. *Environ. Sci. Technol.* **2010**, *44*, 7897–902.
- (10) Zhang, D.; Zhang, R. Ozonolysis of  $\alpha$ -Pinene and  $\beta$ -Pinene: Kinetics and Mechanism. *J. Chem. Phys.* **2005**, *122*.
- (11) Claeys, M.; Graham, B.; Vas, G.; Wang, W.; Vermeylen, R.; Pashynska, V.; Cafmeyer, J.; Guyon, P.; Andreae, M. O.; Artaxo, P.; et al. Formation of Secondary Organic Aerosols through Photo-oxidation of Isoprene. *Science* **2004**, *303*, 1173–6.
- (12) Yu, J. Z.; Cocker, D. R.; Griffin, R. J.; Flagan, R. C.; Seinfeld, J. H. Gas-Phase Ozone Oxidation of Monoterpenes: Gaseous and Particulate Products. *J. Atmos. Chem.* **1999**, *34*, 207–58.
- (13) Pöschl, U. Atmospheric Aerosols: Composition, Transformation, Climate and Health Effects. *Angew. Chem.* **2005**, *44*, 7520–40.
- (14) Ebben, C. J.; Shrestha, M.; Martinez, I. S.; Corrigan, A. L.; Frossard, A. A.; Song, W. W.; Worton, D. R.; Petäjä, T.; Williams, J.; Russell, L. M.; et al. Organic Constituents on the Surfaces of Aerosol Particles from Southern Finland, Amazonia, and California Studied by Vibrational Sum Frequency Generation. *J. Phys. Chem. A* **2012**, *116*, 8271–90.
- (15) Seinfeld, J. H.; Pandis, S. N. *Atmospheric Chemistry and Physics*; John Wiley & Sons: New York, 1998.
- (16) Finlayson-Pitts, B.; Pitts, J. *Chemistry of the Upper and Lower Atmosphere: Theory, Experiments, and Applications*; Academic Press: San Diego, CA, 2000.
- (17) Barnum, T. J.; Medeiros, N.; Hinrichs, R. Z. Condensed-Phase versus Gas-Phase Ozonolysis of Catechol: A Combined Experimental and Theoretical Study. *Atmos. Environ.* **2012**, *55*, 98–106.
- (18) Pillar, E. A.; Camm, R. C.; Guzman, M. I. Catechol Oxidation by Ozone and Hydroxyl Radicals at the Air–Water Interface. *Environ. Sci. Technol.* **2014**, *48*, 14352–60.
- (19) Stokes, G. Y.; Buchbinder, A. M.; Gibbs-Davis, J. M.; Scheidt, K. A.; Geiger, F. M. Heterogeneous Ozone Oxidation Reactions of 1-Pentene, Cyclopentene, Cyclohexene, and Menthenol Derivative Studied by Sum Frequency Generation. *J. Phys. Chem. A* **2008**, *112*, 11688–98.
- (20) Stokes, G. Y.; Chen, E. H.; Buchbinder, A. M.; Paxton, W. F.; Keeley, A.; Geiger, F. M. Atmospheric Heterogeneous Stereochemistry. *J. Am. Chem. Soc.* **2009**, *131*, 13733–7.
- (21) Hopkins, A. J.; McFearin, C. L.; Richmond, G. L. SAMs under Water: The Impact of Ions on the Behavior of Water at Soft Hydrophobic Surfaces. *J. Phys. Chem. C* **2011**, *115*, 11192–203.
- (22) Moussa, S. G.; McIntire, T. M.; Szoeri, M.; Roeselova, M.; Tobias, D. J.; Grimm, R. L.; Hemminger, J. C.; Finlayson-Pitts, B. J. Experimental and Theoretical Characterization of Adsorbed Water on Self-Assembled Monolayers: Understanding the Interaction of Water with Atmospherically Relevant Surfaces. *J. Phys. Chem. A* **2009**, *113*, 2060–9.
- (23) Burden, D. K.; Johnson, A. M.; Krier, J. M.; Nathanson, G. M. The Entry of HCl through Soluble Surfactants on Sulfuric Acid: Effects of Chain Branching. *J. Phys. Chem. B* **2014**, *118*, 7993–8001.
- (24) Ebben, C. J.; Martinez, I. S.; Shrestha, M.; Buchbinder, A.; Corrigan, A. L.; Guenther, A.; Karl, T.; Petäjä, T.; Song, W. W.; Zorn, S. R.; et al. Contrasting Organic Aerosol Particles from Boreal and Tropical Forests During Humppa-Copec2010 and Amaze-08 Using Coherent Vibrational Spectroscopy. *Atmos. Chem. Phys.* **2011**, *11*, 10317–29.
- (25) Ebben, C. J.; Zorn, S. R.; Lee, S.-B.; Artaxo, P.; Martin, S. T.; Geiger, F. M. Stereochemical Transfer to Atmospheric Aerosol Particles Accompanying the Oxidation of Biogenic Volatile Organic Compound. *Geophys. Res. Lett.* **2011**, *38*, L16807–11.
- (26) Ebben, C. J.; Strick, B. F.; Upshur, M. A.; Chase, H. M.; Achtyl, J. L.; Thomson, R. J.; Geiger, F. M. Towards the Identification of Molecular Constituents Associated with the Surfaces of Isoprene-Derived Secondary Organic Aerosol (SOA) Particles. *Atmos. Chem. Phys.* **2014**, *14*, 2303–14.
- (27) Shrestha, M.; Zhang, Y.; Ebben, C. J.; Martin, S. T.; Geiger, F. M. Vibrational Sum Frequency Generation Spectroscopy of Secondary

Organic Material Produced by Condensational Growth from  $\alpha$ -Pinene Ozonolysis. *J. Phys. Chem. A* **2013**, *117*, 8427–36.

(28) Frederiker, M. L.; Achtyl, J. L.; Knowles, K. E.; Weiss, E. A.; Geiger, F. M. Surface Amplified Ligand Disorder in CdSe Quantum Dots Determined by Electron and Coherent Vibrational Spectroscopy. *J. Am. Chem. Soc.* **2011**, *133*, 7476–81.

(29) Bordenyuk, A. N.; Weeraman, C.; Yatawara, A.; Jayathilake, H. D.; Stioipkin, I.; Liu, Y.; Benderskii, A. V. Vibrational Sum Frequency Generation Spectroscopy of Dodecanethiol on Metal Nanoparticles. *J. Phys. Chem. C* **2007**, *111*, 8925–33.

(30) Walter, S. R.; Youn, J.; Emery, J. D.; Kewalramani, S.; Hennek, J. W.; Bedzyk, M. J.; Facchetti, A.; Marks, T. J.; Geiger, F. M. In-Situ Probe of Gate Dielectric-Semiconductor Interfacial Order in Organic Transistors: Origin and Control of Large Performance Sensitivities. *J. Am. Chem. Soc.* **2012**, *134*, 11762–33.

(31) Baker, L. R.; Kennedy, G.; Krier, J. M.; van Spronson, M.; Onorato, R. M.; Somorjai, G. A. The Role of an Organic Cap in Nanoparticle Catalysis: Reversible Restructuring of Carbonaceous Material Controls Catalytic Activity of Platinum Nanoparticles for Ethylene Hydrogenation and Methanol Oxidation. *Catal. Lett.* **2012**, *142*, 1286–94.

(32) Lu, Z.; Karakoti, A.; Velarde, L.; Wang, W.; Yang, P.; Thevuthasan, S.; Wang, H.-f. Dissociative Binding of Carboxylic Acid Ligand on Nanoceria Surface in Aqueous Solution: A Joint in Situ Spectroscopic Characterization and First-Principles Study. *J. Phys. Chem. C* **2013**, *117*, 24329–38.

(33) Sefer, G. A.; Du, Q.; Miranda, P. B.; Shen, Y. R. Surface Crystallization of Liquid *N*-Alkanes and Alcohol Monolayers Studied by Surface Vibrational Spectroscopy. *Chem. Phys. Lett.* **1995**, *235*, 347–54.

(34) Wang, J.; Woodcock, S. E.; Buck, S. M.; Chen, C.; Chen, Z. Different Surface-Restructuring Behaviors of Poly(Methacrylate) S Detected by SFG. *J. Am. Chem. Soc.* **2001**, *123*, 9470–1.

(35) Robertson, E. J.; Carpenter, A. P.; Olson, C. M.; Ciszewski, R. K.; Richmond, G. L. Metal Ion Induced Adsorption and Ordering of Charged Macromolecules at the Aqueous/Hydrophobic Liquid Interface. *J. Phys. Chem. C* **2014**, *118*, 15260–73.

(36) Epstein, S. A.; Blair, S. L.; Nizkorodov, S. A. Direct Photolysis of  $\alpha$ -Pinene Ozonolysis Secondary Organic Aerosol: Effect on Particle Mass and Peroxide Content. *Environ. Sci. Technol.* **2014**, *48*, 11251–8.

(37) Liu, P.; Zhang, Y.; Martin, S. T. Complex Refractive Indices of Thin Films of Secondary Organic Materials by Spectroscopic Ellipsometry from 220 to 1200 nm. *Environ. Sci. Technol.* **2013**, *47*, 13594–601.

(38) Ebben, C. J.; Ault, A. P.; Ruppel, M. J.; Ryder, O. S.; Bertram, T. H.; Grassian, V. H.; Prather, K. A.; Geiger, F. M. Size-Resolved Sea Spray Aerosol Particles Studied by Vibrational Sum Frequency Generation. *J. Phys. Chem. A* **2013**, *117*, 6589–601.

(39) Velarde, L.; Zhang, X.-y.; Lu, Z.; Joly, A. G.; Wang, Z.; Wang, H.-f. Communication: Spectroscopic Phase and Lineshapes in High-Resolution Broadband Sum Frequency Vibrational Spectroscopy: Resolving Interfacial Inhomogeneities of “Identical” Molecular Groups. *J. Chem. Phys.* **2011**, *135*.

(40) Hayes, P. L.; Chen, E. H.; Achtyl, J. L.; Geiger, F. M. An Optical Voltmeter for Studying Cetyltrimethylammonium Interacting with Fused Silica/Aqueous Interfaces at High Ionic Strength. *J. Phys. Chem. A* **2009**, *113*, 4269–4280.

(41) Velarde, L.; Wang, H.-f. Unified Treatment and Measurement of the Spectral Resolution and Temporal Effects in Frequency-Resolved Sum-Frequency Generation Vibrational Spectroscopy (SFG-VS). *Phys. Chem. Chem. Phys.* **2013**, *15*, 19970–84.

(42) Shen, Y. R. *The Principles of Nonlinear Optics*; John Wiley & Sons: New York, 1984.

(43) Geiger, F. M. Second Harmonic Generation, Sum Frequency Generation, and C(3): Dissecting Environmental Interfaces with a Nonlinear Optical Swiss Army Knife. *Annu. Rev. Phys. Chem.* **2009**, *60*, 61.

(44) Richmond, G. L. Structure and Bonding of Molecules at Aqueous Surfaces. *Annu. Rev. Phys. Chem.* **2001**, *52*, 357–89.

(45) Eisenthal, K. Liquid Interfaces Probed by Second-Harmonic and Sum-Frequency Spectroscopy. *Chem. Rev.* **1996**, *96*, 1343–60.

(46) Mifflin, A. L.; Velarde, L.; Ebben, C. J.; Upshur, M. A.; Lu, Z.; Strick, B. F.; Thomson, R. J.; Wang, H.-F.; Geiger, F. M. Sub-1 cm<sup>-1</sup> Resolution Sum Frequency Generation Vibrational Spectra of  $\alpha$ -Pinene. 2014, submitted.

(47) Shultz, M. J.; Baldelli, S.; Schnitzer, C.; Simonelli, D. Aqueous Solution/Air Interfaces Probed with Sum Frequency Generation Spectroscopy. *J. Phys. Chem. B* **2002**, *106*, 5313–24.

(48) Stioipkin, I. V.; Weeraman, C.; Pieniazek, P. A.; Shalhout, F. Y.; Skinner, J. L.; Benderskii, A. V. Hydrogen Bonding at the Water Surface Revealed by Isotopic Dilution Spectroscopy. *Nature* **2011**, *474*, 192–5.

(49) Mondal, J. A.; Nihongyanagi, S.; Yamaguchi, S.; Tahara, T. Three Distinct Water Structures at a Zwitterionic Lipid/Water Interface Revealed by Heterodyne-Detected Vibrational Sum Frequency Generation. *J. Am. Chem. Soc.* **2012**, *134*, 7842–50.

(50) Chen, X.; Hua, W.; Huang, Z.; Allen, H. C. Interfacial Water Structure Associated with Phospholipid Membranes Studied by Phase-Sensitive Vibrational Sum Frequency Generation Spectroscopy. *J. Am. Chem. Soc.* **2010**, *132*, 11336–42.

(51) Hill, P. G.; MacMillan, R. D. Saturation States of Heavy Water. *J. Phys. Chem. Ref. Data* **1980**, *9*, 735–49.

(52) Matsunga, N.; Nagashima, A. Saturation Vapor Pressure and Critical Constants of H<sub>2</sub>O, D<sub>2</sub>O, T<sub>2</sub>O, and Their Isotopic Mixtures. *Int. J. Thermom.* **1987**, *8*, 681–94.

(53) Stone, J. A.; Zimmerman, J. H. Index of Refraction of Air, Engineering Metrology Toolbox. <http://emtoolbox.nist.gov/Wavelength/Ciddor.asp> (accessed 2014).

(54) Alonso, M.; Finn, E. J. *Physik*; Addison-Wesley: Bonn, 1988.

(55) Buchbinder, A. M.; Weitz, E.; Geiger, F. M. Pentane, Hexane, Cyclopentane, Cyclohexane, 1-Hexene, 1-Pentene, Cis-2-Pentene, Cyclohexene, and Cyclopentene at Vapor/ $\alpha$ -Alumina and Liquid/ $\alpha$ -Alumina Interfaces Studied by Broadband Sum Frequency Generation. *J. Phys. Chem. C* **2010**, *114*, 554–66.

(56) Varutbangkul, V.; Brechtel, F. J.; Bahreini, R.; L, N. N.; Keywood, M. D.; Kroll, J. H.; Flagan, R. C.; Seinfeld, J. H.; Lee, A.; Goldstein, A. H. Hygroscopicity of Secondary Organic Aerosols Formed by Oxidation of Cycloalkenes, Monoterpenes, Sesquiterpenes, and Related Compounds. *Atmos. Chem. Phys.* **2006**, *6*, 2367–88.

(57) Wex, H.; Petters, M. D.; Carrico, C. M.; Hallbauer, E.; Massling, A.; McMeeing, G. R.; Poulain, L.; Wu, Z.; Kreidenweis, S. M.; Stratmann, F. Towards Closing the Gap between Hygroscopic Growth and Activation for Secondary Organic Aerosol: Part 1—Evidence from Measurements. *Atmos. Chem. Phys.* **2009**, *9*, 3987–97.

(58) Buchbinder, A. M.; Weitz, E.; Geiger, F. M. When the Solute Becomes the Solvent: Orientation, Ordering, and Structure of Binary Mixtures of 1-Hexanol and Cyclohexane over the (0001) Alpha-Alumina Surface. *J. Am. Chem. Soc.* **2010**, *132*, 14661–8.

(59) Heaton, K. J.; Sleighter, R. L.; Hatcher, P. G.; Hall, W. A.; Johnston, M. V. Composition Domains in Monoterpene Secondary Organic Aerosol. *Environ. Sci. Technol.* **2009**, *43*, 7797–802.

(60) Li, Y. J.; Chen, Q.; Guzman, M. I.; Chan, C. K.; Martin, S. T. Second-Generation Products Contribute Substantially to the Particle-Phase Organic Material Produced by B-Caryophyllene Ozonolysis. *Atmos. Chem. Phys.* **2011**, *11*, 121–32.

(61) Ehn, M.; Kleist, E.; Junninen, H.; Petäjä, T.; Lönn, G.; Schobesberger, S.; Dal Maso, M.; Trimborn, A.; Kulmala, M.; Worsnop, D. R.; et al. Gas Phase Formation of Extremely Oxidized Pinene Reaction Products in Chamber and Ambient Air. *Atmos. Chem. Phys.* **2012**, *12*, 4589–625.

(62) Ehn, M.; Thornton, J. A.; Kleist, E.; Sipila, M.; Junninen, H.; Pullinen, I.; Springer, M.; Rubach, F.; Tillmann, R.; Lee, B.; et al. A Large Source of Low-Volatility Secondary Organic Aerosol. *Nature* **2014**, *506*, 476–9.

(63) Albitzer, M. A.; Crooks, R. M.; Zaera, F. Adsorption of Carbon Monoxide on Dendrimer-Encapsulated Platinum Nanoparticles: Liquid versus Gas Phase. *J. Phys. Chem. Lett.* **2010**, *1*, 38–40.

(64) Prather, K. A.; Bertram, T. H.; Grassian, V. H.; Deane, G. B.; Stokes, M. D.; DeMott, P. J.; Aluwihare, L. I.; Palenik, B. P.; Azam, F.; Seinfeld, J. H.; et al. Bringing the Ocean into the Laboratory to Probe the Chemical Complexity of Sea Spray Aerosol. *Proc. Natl. Acad. Sci. U.S.A.* **2013**, *110*, 7550–5.

(65) Kim, M. J.; Farmer, D. K.; Bertram, T. H. A Controlling Role for the Air–Sea Interface in the Chemical Processing of Reactive Nitrogen in the Coastal Marine Boundary Layer. *Proc. Natl. Acad. Sci. U.S.A.* **2014**, *111*, 3943–8.

#### ■ NOTE ADDED AFTER ASAP PUBLICATION

This article posted asap on January 22, 2015. The references have been revised in the following locations: Experimental Section, paragraph 3, sentence 1; paragraph 4, sentence 3, paragraph 5, sentence 6. Results section, paragraph 1, sentence 4, paragraph 4, sentence 4. Discussion and Atmospheric Implications section, paragraph 2, sentence 3; paragraph 3, sentence 6. The correct version posted on January 23, 2015.